

Self-Aligned Crossbar for Memristive Device Fabrication (May 2014)

E. Pethybridge

Abstract—Shadow evaporation is demonstrated as a means of producing self-aligned crossbar structures with potential memristive applications. This serves as a solution to difficult metal oxide etching processes by substituting them with a single liftoff to form both electrodes. SEM and STEM analysis confirm the proper formation of the device and highlight opportunities for process optimization. The most significant improvement area is the replacement of tantalum with aluminum for electrode material to prevent oxidation. The shadow evaporation process and device formation are the focus of this exercise.

Index Terms—Crossbar, Memristor, Self-aligned, Shadow Evaporation, SEM

I. INTRODUCTION

The memristor is a device first theorized by Leon Chua in 1971 which is described as a passive two terminal component coupling electrical charge and magnetic flux. This element is referred to as the fourth passive circuit element, completing the conceptual symmetry associated with the resistor, inductor, and capacitor [1].

Memristors are a type of Resistive Random Access Memory (RRAM). RRAM is a form of non-volatile memory currently under development by a number of memory manufacturing companies. In RRAM, the resistance of the element depends on the history of the biasing conditions applied to it. In its simplest representation, it is a resistor with memory.

RRAM is considered to be a contender for next generation memory alternatives due to its compatibility with low voltage operation. Current incumbent NAND and NOR flash technologies require high voltages to set or reset charge storage devices. Using high voltage is disadvantageous for low power applications such as those in the rapid growing mobile market.

A memristor is comprised of two electrodes with an active element placed in between. This simple representation of the device is compatible with a self-aligned shadow evaporation based process. Shadow evaporation exploits the unidirectional nature of thermal evaporation to prevent deposition on select areas of the substrate. This presents a unique opportunity when that can be adapted to device fabrication. In this exercise, such a process is discussed that takes advantage of this potential.

II. THEORY

A. Memristors

Materials such as oxygen depleted metal oxides serve as excellent memristive materials. Oxygen vacancies in these materials serve as quasi-mobile ionic donors which are responsible for the resistive state changes in the device.

When an electrode is placed on either end of a memristive material, it can be biased such that these vacancies rearrange. A low resistance (set) state is formed when these vacancies form a semi conductive path in between either electrode. In contrast, a high resistance (reset) state is formed when these vacancies do not favor this orientation. Additionally, a fairly continuous spectrum of resistance states does exist in between these high and low states.

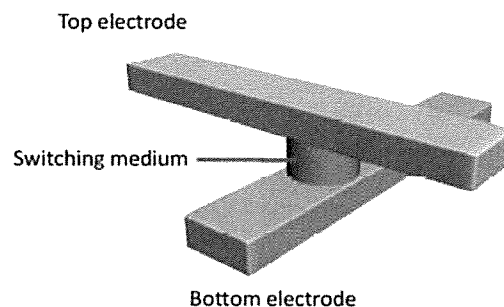


Fig. 1. A basic example of a memristive device. [2]

Because there is a continuous spectrum of resistances associated with each device, it is feasible that multiple bits of information can be stored on a single cell. Despite this, it is difficult to obtain repeatable resistance states that could reliably represent many bits of data. This is due to a semi-random nature of the switching mechanism.

The memory mechanism in a memristor results in observed hysteresis in its I-V characteristics. A voltage sweep is depicted in Fig. 2 where the device starts in its low resistance state. A positive bias is applied and it remains in this low resistance state until the bias is sufficient to rearrange the vacancy positions. Once the vacancies rearrange, the device's resistance increases to a high resistance state until a significant reverse bias is applied. A significant reverse bias changes the state back to its low resistance form.

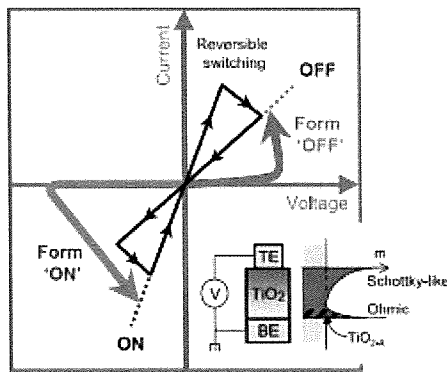


Fig. 2. Memristive I-V Curve [2]. In this characteristic I-V curve, the hysteresis can be observed in the current with respect to voltage.

If managed properly, memristors have true potential to serve in RRAM applications. In order to replace current technologies, they must have sufficiently low read/write times and appropriate data retention (Approximately ten years). In additions to this, they must also overcome several issues related unique to memristive functionality.

B. Shadow Evaporation

One of the key processes in this exercise is the shadow evaporation which is used to self-align the electrodes of the crossbar structure. A shadowed evaporation process takes advantage of the unidirectional nature of evaporation in high vacuum. This process utilizes the aspect ratio of space features in a masking material to prevent deposition on certain parts of the substrate. Based upon the orientation of the wafer, deposition can also be allowed on certain areas. In this manner, two electrodes can be patterned with a single lithography step.

Shadow evaporation is depicted in Figs. 3 and 4. Fig. 3 is a three dimensional representation of a crossbar structure used for this process. Two dimension cross sections of each electrode are depicted in Fig. 4.

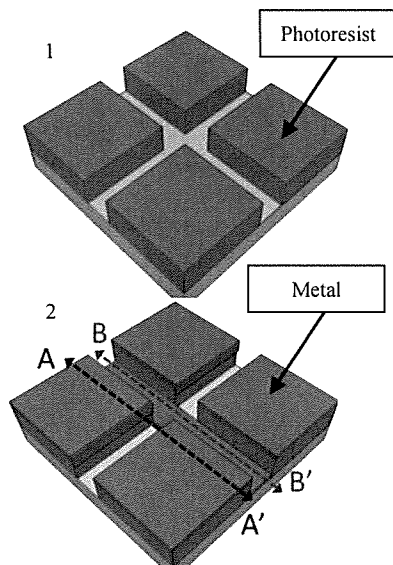


Fig 3. Three Dimensional Shadow Evaporation Representation.

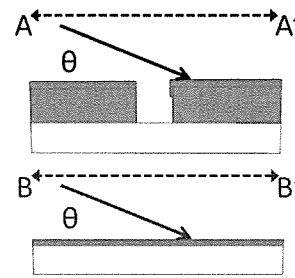


Fig. 4. Shadow Evaporation Cross Section. Metal is evaporated at an angle θ with respect to the substrate. Metal is not deposited on one line (Cross section A), but is deposited on the other line (Cross section B).

Instead of depositing on the wafer surface in some regions (Cross section A in Fig. 4), material deposits on the sidewalls of the masking material. A lower angle of incidence (θ in Fig. 4) means that lower aspect ratio structures can be used to block deposition.

This technique has potential for on chip fabrication of a number of metallic junction devices. Such devices include spin-based electronic devices, superconducting qubits, nanofridges, and single electron transistors [3]. Despite the compatibility with a number of different devices, shadow evaporation has largely remained as a presence in academia over industry.

A shadow evaporation process is particularly advantageous for memristive devices because it involves liftoff so the films do not have to be etched. Difficulties are often encountered in etching memristive films.

III. EXPERIMENTAL SETUP

A. Process Flow

A process has been developed for the R.I.T. Semiconductor and Microsystems Fabrication Laboratory (SMFL) in order to fabricate these memristive devices. Because of the nature of a self-aligned process, the fabrication flow is relatively short with only two lithography levels. An acetone based liftoff is done after both the final electrode deposition and the bond pad deposition. This is done to remove the excess unwanted material as well as the photoresist material.

A second lithography layer was incorporated to prevent parasitic memristor formation at the bottom electrode bond pad. It is also being used to reduce parasitic resistance by increasing the width of the lines connecting either electrode to the bond pad.

Test structures have been formed to confirm the successful execution of the shadow evaporation electrically. Additional test structures have been implemented to determine maximum achievable line density and to observe the shadowing effect over a long distance. These structures were designed to help acquire in line processing data.

The full process flow is detailed in the Appendix. The highlights of the process flow are outline in Fig. 5.

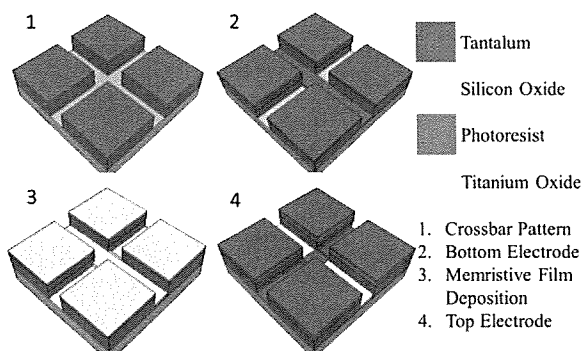


Fig. 5. Memristive Crossbar Fabrication Major Process Steps. After step 4 in the process, a liftoff is performed and then bond pads are defined.

B. Compatibility with R.I.T. SMFL

R.I.T.'s SMFL is well equipped to perform a process as discussed above. Table 2 in the Appendix outlines the equipment necessary to perform this process in a general overview.

Once an isolation oxide was grown across the wafer, the crossbar structures were patterned using an ASML i-line stepper with AZ1518 photoresist. AZ1518 is a thicker coating photoresist which coats at roughly $1.8\ \mu\text{m}$ with a spin speed of 2000 RPM it was selected to produce higher aspect ratio structures that liftoff more readily.

Each shadow evaporation process was performed in a CHA electron beam evaporator. This was selected over a thermal evaporator because it provides much greater film thickness control. Tantalum was used for the electrode material. The titanium oxide was deposited via a reactive sputter using a CVC 601 DC sputtering system with a four inch titanium target. Liftoff was performed using acetone in an ultrasonic wet bench. Bond pads were then defined to connect to the crossbar, completing the process flow.

C. Device Design

Several different device dimensions and test structures were designed to fully characterize the shadow evaporation process in addition to device properties. Crossbar dimensions have been varied from $0.25\ \mu\text{m}$ up to $10\ \mu\text{m}$ and different length bond pads were designed to connect to the crossbar structures. Bond pads were necessary for this exercise to reduce parasitic memristive and resistive components and to test the devices using standard probing methods. Fig. 6 represents the crossbar device design.

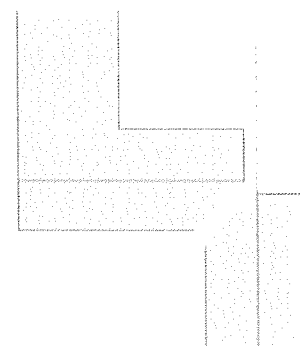


Fig. 6. Crossbar Device Design. Blue represents the bond pad metal and green represents the crossbar structure.

These crossbar structures were also designed in three by three arrays. Test structures were incorporated to test the effectiveness of the cross bar shadowing.



Fig. 7. Electrical test structure design to prevent shorting during the shadow process. Bond pads are surrounded by lines oriented 45 degrees about the direction of evaporation to stop deposition in either direction.

Pinwheels have been included in the layout to investigate the effects of angle tolerance associated with shadow evaporation. In addition to this, density test structures were designed to observe the translation of shadow evaporation to high density arrays.

IV. EXPERIMENTAL RESULTS

Multiple iterations of the earlier steps in the process flow were performed during process development and eventually one wafer was brought to completion. The devices were subjected to electrical analysis as well as imaging analysis including SEM and TEM images.

The effects of shadowing were apparent early in the experiment, even under inspection with a light microscope. Fig. 8 displays a test structure after the first shadow evaporation process.

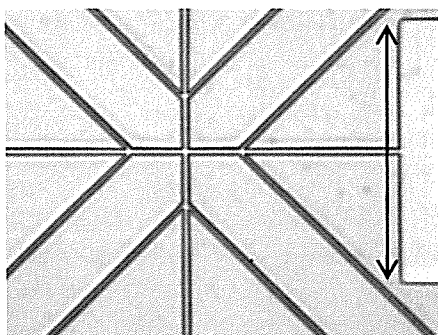


Fig. 8. 1.2 μm Test Structure after First Shadow Evaporation. This is a test structure similar to that designed in Fig. 7. The pink line is the deposited material and green areas are where no material has been deposited. The bond pad is 100 μm in width for reference.

Fig. 9 represent a pinwheel structure with 1.2 μm space widths. It can be seen that there is an approximate 15 degree tolerance for shadowing on either side of the evaporation central axis.

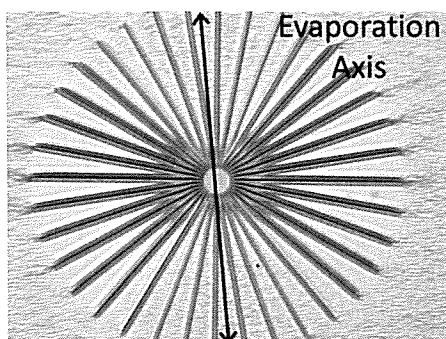
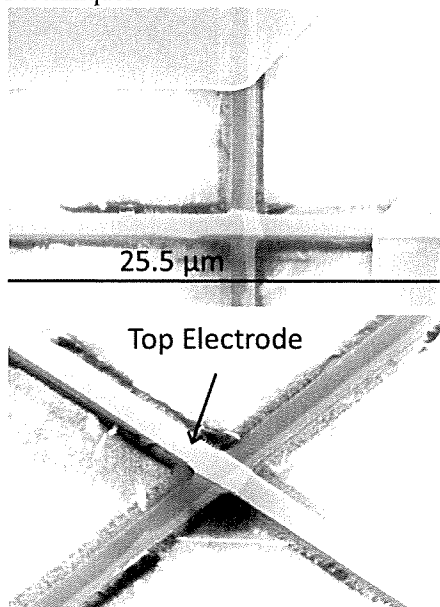


Fig. 9. 1.2 μm Pinwheel. The diameter of the pin wheel is 360 μm . Pink areas represent regions where evaporated material deposited. Hillocks from resist damage are also present in this image.

Although light microscope pictures provide a good preliminary evaluation of the processing success, it is much more valuable to evaluate the self-alignment using more sophisticated techniques.



Figs. 10 and 11. R.I.T. SEM images of 1 μm Crossbar (Top-down View). The

top electrode overlaps the bottom electrode only at the center of the crossbar. Unintentional partial shadowing of the bottom electrode is also apparent. Sidewall material remained after liftoff of the crossbar layers. Line width is approximately 0.5 μm thicker than defined on the photomask.

Figs. 10 and 11 confirm the successfully formation of a crossbar structure but highlight other process related issues. The bottom electrode partially shadowed along its length due to its off center position on the wafer. There is also minor shadowing variation in the top electrode. This would cause issues with reproducibility across the wafer surface.

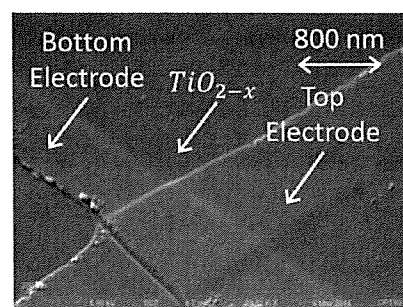
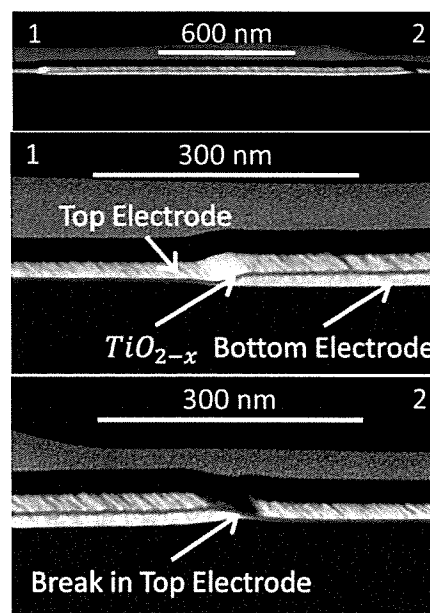


Fig. 12. University of Rochester SEM Image of 1 μm Crossbar (Top-Down View). A clear break in the top electrode is apparent on the edge furthest away from the evaporation source. This depicts shadowing of the top electrode due to the bottom electrode.

The shadowing of the top electrode indicates just how sensitive the shadowing process is. This was anticipated and the device side of the crossbar was placed closest to the electrode.



Figs. 13-15. STEM Results from Micron Technology for 1 μm Crossbar. A top electrode, bottom electrode, and center film are very clearly defined. Grains in the top electrode are observed with an angle resembling the evaporation angle. A break is formed in the top electrode due to shadowing caused by the bottom electrode.

The STEM results in Figs. 13-15 provide conclusive results that the crossbar structure formed and aligned as intended. They also provide evidence supporting that the bottom

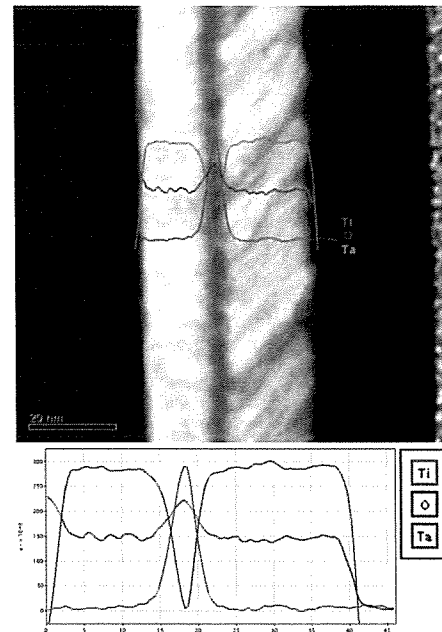
electrode is causing a secondary shadowing effect on the top electrode.

Despite successfully aligning the materials to form a two terminal device, electrical testing yielded open circuits for each device sampled. Further investigation of the material set indicates that the tantalum electrodes oxidized. A quick experiment was performed evaporating tantalum without devices in the reaction chamber. It was found that even with a base pressure of 300 nanoTorr, the tantalum still oxidized during evaporation. An effort was made to reduce the through an aluminothermic reaction; however, the thermal budget was too low to observe any results [4]. Attempts to electroform the contacts also proved unsuccessful.

V. DISCUSSION OF RESULTS

The use of tantalum in the electron beam evaporation for defining the electrodes created several challenges in device fabrication. Due to the low vapor pressure of tantalum, the material had to be heated up to very high temperatures (Approximately 2500 degrees Celsius). This high temperature began to damage the resist in most areas in the chamber as hillocks formed. Initially, this was attributed to solvent outgassing; however, bake times for the resist were doubled and no improvement was seen. One region in the chamber consistently exhibited resistance to this temperature. It is suspected that this is because this location is furthest from the electron beam source. There is also a large amount of metal structure around it which is likely serving as a heat sink to conduct heat away from the wafer. Overall, this reduced the throughput of the evaporation process and resulted in several ruined devices.

The high temperature required to evaporate tantalum also caused a large amount of outgassing of various materials in the chamber. This also proved to be an advantage in controlling the electrode film thickness because the material evaporated very slowly; however, this caused the tantalum to oxidize. The low deposition rate gave the material sufficient time to react with oxygen in the chamber and form an insulating film. This hypothesis was confirmed by measuring the resistance of slides placed at varying distances from the evaporation source. The film on the closest slide which experienced the highest deposition rate was conductive while films that were further away were not conductive.



Figs. 16 and 17. STEM EELS Analysis from Micron Technology for 1 μ m crossbar. All material in the film stack is oxidized including the tantalum electrodes. A definitive stack of three films exists.

Figs. 16 and 17 provide definitive proof that the tantalum electrodes oxidized and also that the crossbar structure exists. The titanium oxide film is a bit thinner than expected measuring about four nm. This under deposition is likely due to film nucleation effects; however, this would have not completely compromised test results if the devices could be accessed.

This shadow evaporation crossbar technique proved to be a plausible means of creating simple two terminal devices. Difficulties arise in the process due to variation in shadowing angle across the wafer surface making this process an unlikely candidate for manufacturing. Non-uniformity leads to highly variable junction areas for the devices which would have a distinct impact on performance. This problem was exacerbated because a very thick photoresist film was used. Issues also arose due to the shadowing of the top electrode against the bottom electrode. This problem would make the formation of device arrays quite difficult. A great deal of optimization would have to be performed in order overcome these challenges.

In order to produce the greatest amount of functioning devices, a few modifications to the process must be made. Firstly, aluminum should be used for the electrode material, eliminating the capability of etching the bond pads but providing a more stable deposition process. The deposition angle should then be reduced to some extent to mitigate the intra-wafer variability associated with the shadowing angle. A more aggressive design of experiment should be performed to characterize the stoichiometry in the memristive film and quantify deposition rates for the reactive sputter process. In order to do this, a better measurement system must be established.

Once the base process has been optimized, lithographical

experiments can be done to obtain the minimum possible feature size and explore the limitations of this process. Optimizing the lithography will also make the density test structures more useful in determining the density scaling capability of this process.

VI. CONCLUSION

A process for the fabrication of self-aligned memristive crossbar structures has been demonstrated using a shadow evaporation technique. Although this process presents significant challenges with reproducibility across a wafer surface, it is well suited for an academic research environment. Difficult etch processes for memristive materials can be circumvented using this liftoff based patterning. Although electrical results were not obtained, the successful alignment of the devices has been confirmed using imaging analysis. Several failure modes for this process have been identified and confirmed using SEM and STEM results as well as electron energy loss spectroscopy (EELS). Process optimizations have been proposed for future use in the R.I.T. SMFL. The primary alteration to the process would be to avoid the use of tantalum altogether, substituting it with a more stable metal such as aluminum. This process provides a simple means of creating two terminal passive devices for materials research.

APPENDIX

Process Flow		
Step	Process	Details
1	RCA Clean	Standard recipe for oxide Growth
2	Isolation Oxidation	Precautionary oxide growth on bare substrate for isolation (> 100 nm)
3	Litho Level 1	Crossbar Structures (Variable Resist Thickness) OIR-620: ~1 μ m SC 1827: 3-5 μ m
4	Shadow Evaporation 1	Bottom Electrode (Evaporation Angle = 20-40 degrees) Metal TBD Target: 20 nm
5	Reactive Sputter	Memristive Material Deposition 15 nm TiO ₂
6	Shadow Evaporation 2	Top Electrode (Evaporation Angle = 20-40 degrees) Metal TBD Target: 20 nm 90 degrees out of phase to Evaporation 1
7	Liftoff 1	Acetone Ultrasonic Liftoff
8	Litho Level 2	Bond Pads OIR-620: 1 μ m
9	Sputter	Bond Pads ~ 150 nm
10	Liftoff 2	Acetone Ultrasonic Liftoff
11	Test	Test

Table 1. Process Flow

CVD	Dry Etch	Lithography	Metrology	PVD	Thermal	Wet Etch
None	GaSonics Asher	SSI Track ASML Stepper	Spectramap Nanospec	CHA e beam evaporator CVC 601	Bruce Furnace	RCA Bench Ultrasonic Bench

Table 2. Necessary R.I.T. SMFL Equipment

Santosh Kurinec, and David MacMahon for their help and support in making this work possible. The knowledge and support provided by Dr. Michael Jackson, Patricia Meller, Sean O'Brien, John Nash, Bruce Tolleson, Rich Battaglia, Alex Mann and Dave Yackoff was instrumental in the progression of this project.

Finally, this work might not have been possible without the guidance of Dr. Sean Rommel and Matthew Filmer.

REFERENCES

- [1] Chua, L. O. Memristor - the missing circuit element. IEEE Trans. Circuit Theory 18, 507-519 (1971).
- [2] Sung Hyun Jo, "Nanoscale Memristive Devices for Memory and Logic Applications", Ph. D dissertation, University of Michigan, 2010.
- [3] Florent, Lococoq, et al. "Junction Fabrication by Shadow Evaporation without a suspended bridge," in IOP Publishing.
- [4] R. A. de Brito, F. F. P. Medeiros, U. U. Gomes, F. A. Costa, A. G. P. Silva, C. Alves Jr. "Production of tantalum by aluminothermic reduction in Plasma Reactor: International Journal of Refractory Metals & Hard Materials Vol. 26 (2008), p. 433
- [5] Xia, Q. et al., "Self-Aligned Memristor Cross-Point Arrays Fabricated with One Nanoimprint Lithography Step," in *Nano Letters*, 2010, pp. 2909-2914.

Eric M. Pethybridge was born in Rochester, New York, in 1991. He is currently pursuing a BS in Microelectronic Engineering from Rochester Institute of Technology and will be graduating in May 2014. During his time at R.I.T., he has completed semiconductor manufacturing related co-ops at Micron Technology and Ortho Clinical Diagnostics where he presently works part time.

Eric has accepted a Materials Processing Professional Development Program role at Northrop Grumman which he will begin after graduation.

ACKNOWLEDGMENT

The author would like to thank my project advisor, Dr.